

BEVTraj: Map-Free End-to-End Trajectory Prediction in Bird's-Eye View with Deformable Attention and Sparse Goal Proposals

Minsang Kong, Myeongjun Kim, Sang Gu Kang, Sang Hun Lee, *Member, IEEE*,

Abstract—In autonomous driving, trajectory prediction is essential for ensuring safe and efficient navigation. To improve prediction accuracy, recent approaches often rely on pre-built high-definition (HD) maps or real-time local map construction modules to incorporate static environmental information. However, pre-built HD maps are limited to specific regions and cannot adapt to transient changes. In addition, local map construction modules, which recognize only predefined elements, may fail to capture critical scene details or introduce errors that degrade prediction performance. To overcome these limitations, we propose Bird's-Eye View Trajectory Prediction (BEVTraj), a novel trajectory prediction framework that operates directly in the bird's-eye view (BEV) space utilizing real-time sensor data without relying on any pre-built maps. The BEVTraj leverages deformable attention to efficiently extract relevant context from dense BEV features. Furthermore, we introduce a Sparse Goal Candidate Proposal (SGCP) module, which enables full end-to-end prediction without requiring any post-processing steps. Extensive experiments demonstrate that the BEVTraj achieves performance comparable to state-of-the-art HD map-based models while offering greater flexibility by eliminating the dependency on pre-built maps. [The source code is available at https://github.com/Kongminsang/bevtraj](https://github.com/Kongminsang/bevtraj).

Index Terms—Trajectory prediction, autonomous vehicles, deep learning, sensor fusion, deformable attention, bird's-eye-view.

I. INTRODUCTION

TRAJECTORY prediction plays a pivotal role in autonomous driving, enabling vehicles to anticipate the future movements of surrounding agents and make safer, more informed decisions. However, this task remains inherently difficult due to the multimodal nature of agent behaviors and the complex interactions between agents and their environments. Accurately modeling these interactions demands a deep understanding of the environment's structural constraints, such as road topology, which provide a critical context for forecasting dynamic behaviors.

Standard-definition (SD) maps provide static information for the vast majority of roads worldwide but lack the precision and semantic richness required for advanced tasks such as

autonomous driving. Recent studies have explored methods to extract static context from high-definition (HD) maps for trajectory prediction, leveraging autonomous driving datasets that include pre-built HD maps. However, reliance on pre-built HD maps presents critical limitations: their high construction costs and labor-intensive maintenance restrict coverage to limited regions and preclude real-time updates. As a result, trajectory prediction methods that depend on these maps are constrained to mapped areas and struggle to adapt to sudden changes in road conditions, such as construction zones or accidents

For these reasons, methods for constructing local HD maps in real time have been proposed, enabling autonomous vehicles to operate in unmapped areas and rapidly adapt to dynamic road conditions [1]–[3]. These real-time HD maps are typically aligned with the ego vehicle's coordinate frame, helping to mitigate failures caused by localization errors. However, if the prediction module relies solely on the outputs from the map construction process, it becomes highly susceptible to misclassification, missing elements, and positional inaccuracies. Moreover, most map construction methods detect only a limited set of predefined classes (e.g., dividers, boundaries, pedestrian crossings) from raw sensor data, which contains a broad range of environmental information. Without incorporating this additional scene context, an autonomous driving system may overlook critical cues that significantly affect trajectory prediction accuracy.

To better leverage available information, it is important to actively utilize raw sensor data for trajectory prediction, as it contains rich semantic and geometric information that is not fully captured by HD maps. However, sensor data is significantly denser and more redundant than vectorized HD maps, necessitating a mechanism to extract only the most relevant information for trajectory prediction. To address this issue, we propose a novel framework, **Bird's-Eye View Trajectory prediction (BEVTraj)**. Rather than relying on pre-built HD maps, BEVTraj constructs Bird's-Eye View (BEV) representations from raw sensor data and directly employs them for trajectory prediction, leveraging deformable attention to extract essential cues from dense BEV features, as illustrated in Fig. 1.

The BEVTraj framework offers several advantages over existing methods. Compared to approaches that rely on HD maps—which provide a high-level abstraction of the driving environment—directly leveraging low-level BEV representations significantly reduces information loss. Additionally, BEVTraj can be seamlessly integrated into modern autonomous driving systems that adopt the BEV paradigm [4]–[6]. By incorporating deformable attention, BEVTraj selec-

Manuscript received July 10, 2025

Minsang Kong and Myeongjun Kim are with the Department of Automobile and IT Convergence, Kookmin University, 77 Jeongneung-ro, Seongbuk-gu, Seoul 02707, Republic of Korea (e-mail: gms0725@kookmin.ac.kr; thd3266772@kookmin.ac.kr).

Sang Gu Kang is with the Department of Automotive Engineering, Kookmin University, 77 Jeongneung-ro, Seongbuk-gu, Seoul 02707, Republic of Korea (e-mail: k84652001@kookmin.ac.kr).

Sang Hun Lee is with the Graduate School of Automobile and Mobility, Kookmin University, 77 Jeongneung-ro, Seongbuk-gu, Seoul 02707, Republic of Korea (e-mail: shlee@kookmin.ac.kr, ORCID: <https://orcid.org/0000-0001-8888-2201>).

Minsang Kong and Myeongjun Kim have contributed equally.

The corresponding author is Sang Hun Lee (e-mail: shlee@kookmin.ac.kr).

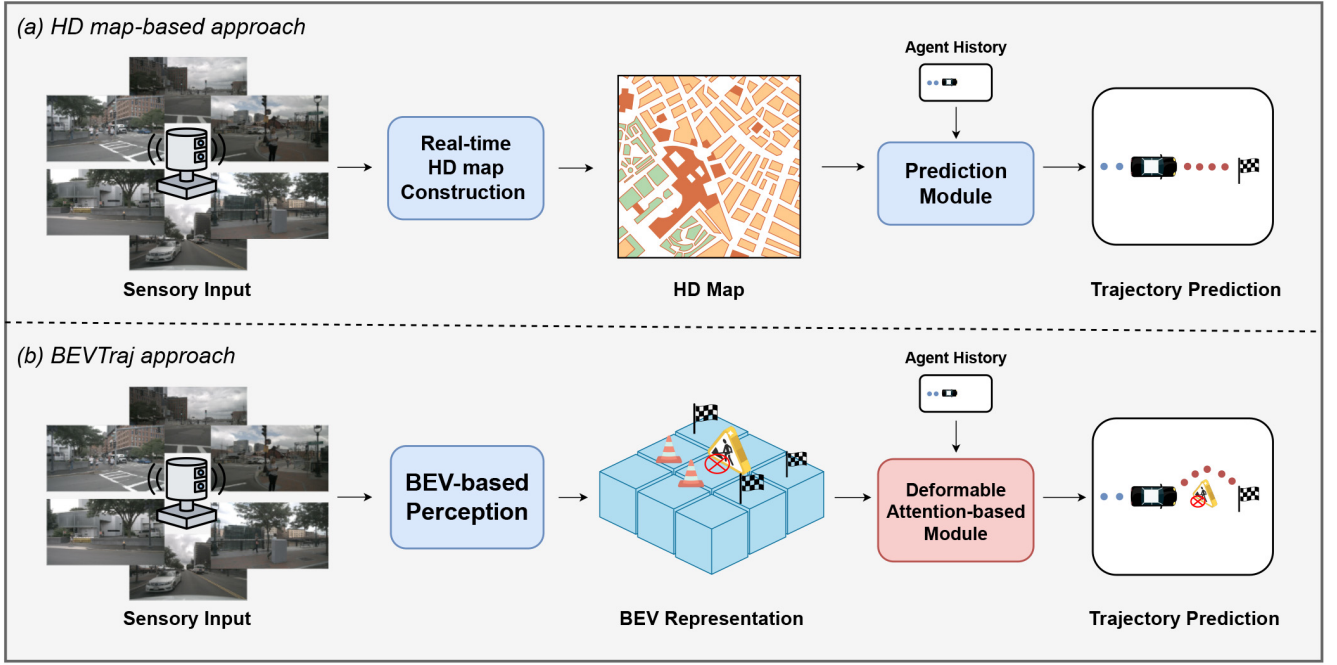


Fig. 1. Two possible approaches for trajectory prediction in the absence of a pre-defined HD map. The first approach (top) constructs an HD map in real time and applies conventional HD map-based prediction methods. The second approach (bottom), proposed in this study as BEVTraj, directly predicts trajectories by leveraging BEV features extracted from raw sensor data.

tively aggregates only the most relevant features for accurate trajectory prediction. Furthermore, we introduce the *Sparse Goal Candidate Proposal (SGCP)* module to address the issue that the density of goal candidates strongly influences the performance of existing goal-based methods. With this module, BEVTraj supports fully end-to-end trajectory prediction without the need for post-processing steps such as non-maximum suppression (NMS). Our contributions are summarized as follows.

- We propose Bird's-Eye View Trajectory Prediction (BEVTraj), a novel goal-driven trajectory prediction framework that directly leverages BEV representations constructed from raw sensor data, thereby eliminating the reliance on pre-built HD maps.
- BEVTraj utilizes low-level BEV feature representations that effectively capture essential scene context while substantially reducing information loss compared to high-level HD maps.
- BEVTraj actively leverages deformable attention across multiple stages to selectively aggregate only the information critical for trajectory prediction, enhancing efficiency and prediction accuracy in dense and redundant BEV representations.
- We introduce the Sparse Goal Candidate Proposal (SGCP) module, which alleviates the sensitivity of goal-based methods to goal candidate density and enables fully end-to-end trajectory prediction without the need for post-processing steps such as non-maximum suppression (NMS).
- Our framework is fully compatible with modern autonomous driving systems adopting the BEV paradigm,

facilitating seamless integration into existing pipelines.

II. RELATED WORK

Many studies have proposed trajectory prediction methods that leverage static information from pre-built HD maps. Early methods employed convolutional neural networks (CNNs) to process rasterized map images, capturing spatial features but suffering from information loss and suboptimal spatial encoding. These limitations rendered CNN-based approaches less effective for trajectory prediction compared to vectorized or graph-based representations, which provide more structured encodings of road layouts and traffic constraints [7]–[12]. With this shift, Transformer-based models have emerged, utilizing self-attention mechanisms [13] to model complex spatial relationships and improve map feature representations [14]–[19]. In particular, HiVT [18] adopts an agent-centric representation, where scene elements are normalized with respect to each agent's coordinate frame to enhance prediction accuracy. In contrast, QCNet [19] adopts a query-centric design, avoiding per-agent normalization and enabling more efficient multi-agent trajectory prediction.

Some approaches adopt *goal-based* methods, where multiple goal candidates are generated to predict multimodal future trajectories, as seen in DenseTNT [20] and MTR (Motion Transformer) [15]. Among them, MTR—most relevant to our work—draws inspiration from Conditional DETR [21] and DAB-DETR [22], assigning initial position embeddings to queries to accelerate training convergence. It also introduces a novel decoder structure that formulates motion prediction as a joint optimization problem of global intention localization and local movement refinement through motion query pairs.

Like MTR, R-Pred refines initial trajectory predictions using a Tube-Query Attention-based refinement module [23]. Similarly, BEVTraj adopts an iterative refinement process, enabling more flexible and efficient goal candidate selection.

As mentioned in Section I, pre-built HD maps are costly to construct and often insufficient for real-world autonomous driving, which has motivated research on local HD map construction to automate the mapping process [1]–[3]. However, errors in map construction—such as misclassifications or omissions—can degrade the performance of downstream tasks, including trajectory prediction and path planning. To address errors in upstream components such as detection and tracking, recent studies have explored unified frameworks that directly perform decision-making [24]–[27]. While some of these models incorporate trajectory prediction, others focus solely on planning, treating prediction as an implicit component rather than a standalone task.

Another line of research adopts a joint perception and prediction approach, aiming to overcome the limitations of traditional map construction and perception pipelines [28]–[30]. By integrating multi-sensor data, these methods enhance environmental perception and improve the stability of trajectory prediction, ultimately supporting more reliable planning and decision-making. In a similar spirit, our method directly predicts future trajectories from raw sensor inputs. In contrast to previous approaches that tightly couple instance segmentation with motion prediction, we assume that a perception pipeline for detection and tracking has already been executed to obtain the historical trajectories of surrounding agents. This design approach enables robust, map-free trajectory prediction by decoupling perception and prediction while maintaining compatibility with standard detection and tracking pipelines.

III. METHOD

In this section, we present BEVTraj, a framework that predicts the multimodal future distribution of the target agent’s trajectory. BEVTraj comprises two main modules: *Scene Context Encoder*, and *Iterative Deformable Decoder*. The Scene Context Encoder generates *scene-level context features* by capturing complex interactions within the scene, utilizing the historical states of agents and the BEV features extracted from raw sensor data. Finally, the Iterative Deformable Decoder sequentially predicts multiple goal candidates and their corresponding initial trajectories for the target agent, and refines these predictions iteratively. An overview of BEVTraj is shown in Fig. 2.

A. Scene Context Encoder

A clear understanding of complex interactions within the scene context is crucial for trajectory prediction. Motion Transformer (MTR) [15] encodes scene context by utilizing a PointNet-like [31] polyline encoder to vectorize road maps and agent trajectories, applying local self-attention to preserve spatial locality and enhance memory efficiency, and using an auxiliary regression head to predict dense future trajectories of surrounding agents to improve interaction modeling. The Scene Context Encoder builds upon this design and introduces

three sub-modules: *Sensor Encoder*, *Pre-Encoder*, and *BEV Deformable Aggregation (BDA)* modules.

1) *Sensor Encoder*: As in object detection, both semantic and geometric information are essential for trajectory prediction, motivating BEVTraj to adopt a sensor fusion architecture that integrates images and point clouds. This raises a critical question: which spatial domain is best suited for representing essential features? BEVTraj adopts the BEV space for the following reasons. First, since trajectory prediction is conducted in BEV space, this alignment ensures consistency between the prediction output and the feature representation. Moreover, Liu et al. [6] argued that lidar point clouds and camera images are fundamentally different modalities and that fusing them in BEV space is the most appropriate approach. Based on these insights, BEVTraj employs BEVFusion [6]—an off-the-shelf sensor fusion architecture—as the Sensor Encoder to generate a BEV feature map $\mathbf{B} \in \mathbb{R}^{C \times H \times D}$, where H and D denote the spatial dimensions. The BEVFusion module can easily be replaced with any other BEV-based fusion model.

The BEV representation differs from HD maps in several respects. HD maps provide high-level abstractions of static elements (e.g., *dividers*, *boundaries*, and *pedestrian crossings*). In contrast, BEV representations derived from raw sensor data contain redundant and often irrelevant information due to the dense, image-like nature of the BEV grid. Therefore, BEVTraj adopts a strategy that aggregates scene information from \mathbf{B} using deformable attention [32], which dynamically computes offsets to identify key points, enabling the model to selectively extract features essential for trajectory prediction. Sections III-B and III-C provide detailed descriptions of how deformable attention is applied to \mathbf{B} for different purposes.

2) *Pre-Encoder*: Previous studies categorize scene interaction encoding into two approaches: preserving or compressing the temporal dimension. The former allows for temporal positional encoding and better captures motion tendencies. In contrast, the latter compresses the temporal axis, improving parameter efficiency by increasing representational capacity with the same number of parameters. MTR adopts the latter approach, which limits its ability to model motion dynamics. To address this limitation, the Scene Context Encoder incorporates a Pre-Encoder that applies temporal self-attention (as introduced by Girgis et al. [14]) prior to temporal dimension. enables more effective modeling of motion tendencies before local self-attention is applied. Furthermore, social self-attention (also introduced by Girgis et al. [14]) follows temporal self-attention to capture inter-agent interactions at each timestep. Finally, a PointNet-like encoder transforms the representation from $\mathbb{R}^{N_a \times t \times d}$ into an *agent feature map* $\mathbf{A} \in \mathbb{R}^{N_a \times D}$, where N_a denotes the number of agents in the scene and t represents the number of past temporal steps.

3) *BEV Deformable Aggregation*: Unlike MTR, which relies on pre-built HD maps, BEVTraj encodes road topology and physical constraints from raw sensor data into BEV feature map \mathbf{B} . In the process of scene context encoding, it is essential to consider not only agent interactions but also these structural constraints. However, due to the high computational cost, global attention—which computes attention scores across all spatial locations—is infeasible on \mathbf{B} . To address this, we

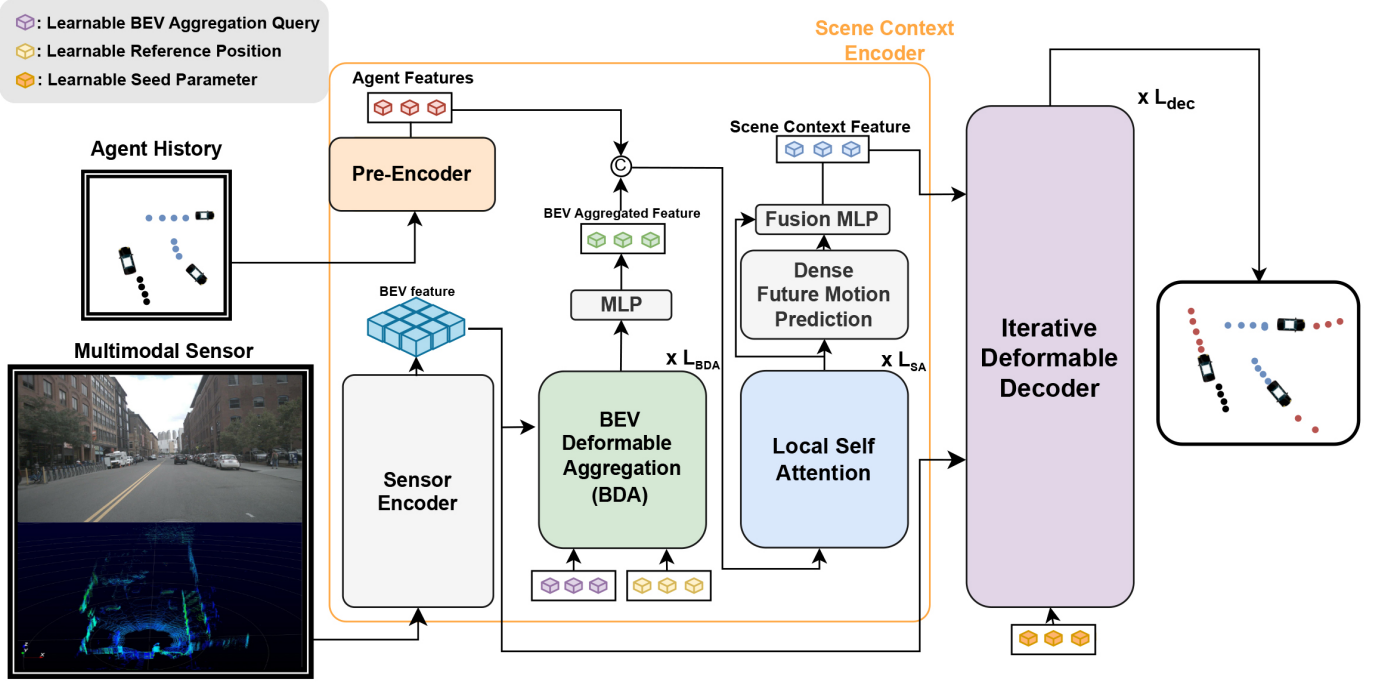


Fig. 2. Overall architecture of BEVTraj. Sensor Encoder processes multimodal sensor data (e.g., camera images, LiDAR point clouds) to generate BEV feature, while Pre-Encoder captures agent motion history. BEV Deformable Aggregation (BDA) module efficiently compresses BEV feature into a compact representation, which is then integrated with Pre-Encoder’s output through local self-attention. Iterative Deformable Decoder predicts the target agent’s trajectory and iteratively refines it using both BEV feature and scene context feature.

propose the *BEV Deformable Aggregation (BDA)* module, which selectively attends to a compact set of key spatial locations in \mathbf{B} and aggregates them into a fixed number of vectors, referred to as the *BEV aggregated feature* $\in \mathbb{R}^{N_m \times D}$. Here, N_m denotes the number of selected spatial locations in the BEV feature map used for aggregation, thereby enabling computationally efficient attention operations.

The structure of BDA is inspired by DAB-Deformable-DETR [22], [32], as illustrated in Fig. 3. BDA is structured around a BEV Aggregate (BA) queries, initialized as zero, and learnable reference positions, which are randomly initialized and processed with sinusoidal positional encoding followed by a multi-layer perceptron (MLP) to obtain positional embeddings. These embeddings are added element-wise to the BA queries and passed through a self-attention layer. In the deformable cross-attention step, the BA queries interacts with the BEV feature map \mathbf{B} , leveraging the learnable reference positions as anchor points to adaptively aggregate spatial information. A lightweight MLP head then computes offsets, which are used to update the reference positions. This process is repeated across multiple layers, progressively refining both the BA queries and their associated reference positions. Finally, the refined BA queries are passed through a final MLP to produce BEV aggregated feature.

By adopting this *position-based iterative refinement* structure, BDA offers the following advantages: (1) It allows reference points to continuously refine their spatial locations based on aggregated BEV information, ensuring that each BA query attends to a specific spatial region while dynamically adapting its position to the underlying data distribution. (2)

This adaptability further facilitates the integration of local self-attention, as introduced in MTR, by providing explicit spatial anchors for each scene element. Notably, the normalized reference points are transformed into the target agent’s coordinate frame, accounting for both the ego vehicle’s state (position and orientation) and the predefined coverage area of \mathbf{B} .

The BEV aggregated feature produced by BDA is then concatenated with the agent feature map \mathbf{A} generated by Pre-Encoder, followed by local self-attention. Subsequently, dense future motion prediction is performed for each agent to account for interactions across future trajectories, resulting in the construction of the *scene context feature* $\mathbf{C} \in \mathbb{R}^{N_a \times D}$.

B. Iterative Deformable Decoder

The *Iterative Deformable Decoder* predicts and refines the multimodal future trajectory of the target agent based on \mathbf{B} and \mathbf{C} , as illustrated in Fig. 4. It comprises three sub-modules: *Sparse Goal Candidate Proposal*, *Initial Trajectory Prediction*, and *Iterative Trajectory Refinement*. Each module employs deformable attention [32] to efficiently process the dense BEV representation. For simplicity, residual connections, normalization layers, feedforward networks, and some MLP components within the decoder are omitted in the following descriptions.

1) *Sparse Goal Candidate Proposal*: As illustrated in Fig. 5, DenseTNT [20] produces dense goal candidates along lanes, while Motion TRansformer (MTR) [15] predefines intention points via k-means clustering on training data. We argue that both approaches require many goal candidates because they do not account for the dynamic state of the target agent or structural constraints when generating goals. To address this, we

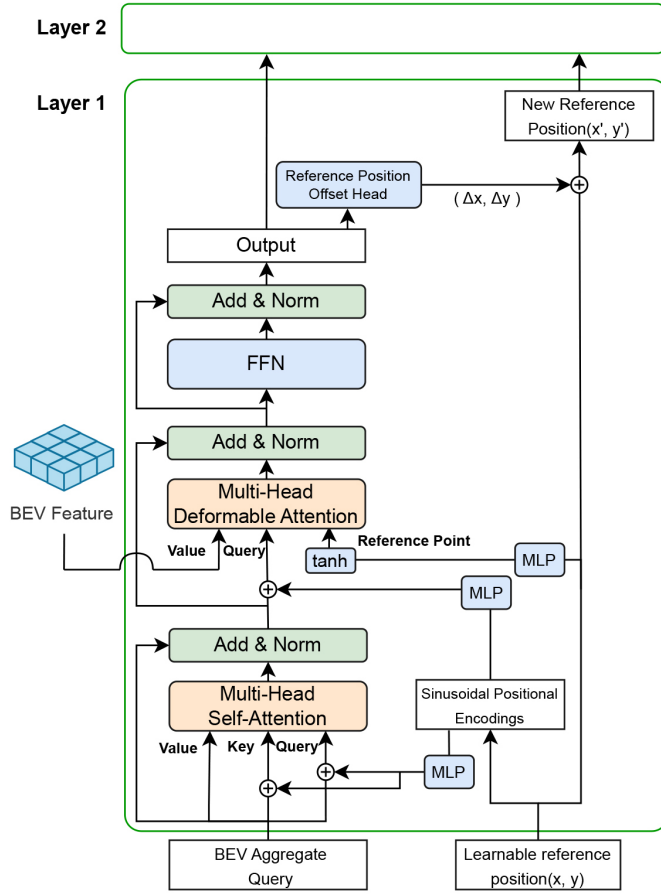


Fig. 3. Architecture of the BEV Deformable Aggregation (BDA) module. The BA queries and learnable reference positions are iteratively refined through self-attention and deformable cross-attention layers. The final BA queries are passed through an MLP to produce BEV aggregated features.

propose the *Sparse Goal Candidate Proposal (SGCP)* module, which predicts a sparse set of K goal candidates—significantly fewer than in prior methods—conditioned on the target agent’s dynamic state $s \in \mathbb{R}^{t \times K_{attr}}$ and the BEV feature map B .

SGCP adopts learnable seed parameters $P \in \mathbb{R}^{K \times D}$ to capture the multimodal behavior of the target agent. In this formulation, each vector in P encodes a distinct driving intention, enabling SGCP to generate diverse goal locations corresponding to different behavior modes. SGCP operates as follows. First, P are fused with dynamic states via an MLP, and the resulting output is processed through deformable cross-attention with the BEV feature map B , producing mode-specific queries $Q_m \in \mathbb{R}^{K \times D}$. Next Q_m is again fused with s through an MLP and refined via self-attention to generate a content query $Q_c \in \mathbb{R}^{K \times D}$. Finally, a lightweight MLP head is applied to Q_c to predict K goal coordinates $\in \mathbb{R}^{K \times 2}$.

Each block in SGCP follows this pipeline and can be stacked multiple times, progressively refining both Q and the predicted goal candidates.

Notably, when performing deformable cross-attention with B , both the reference points and offsets are derived from the key—namely, the BEV feature map B —rather than the query. Since P does not encode any road structure information, deriving sampling locations from B is more appropriate for

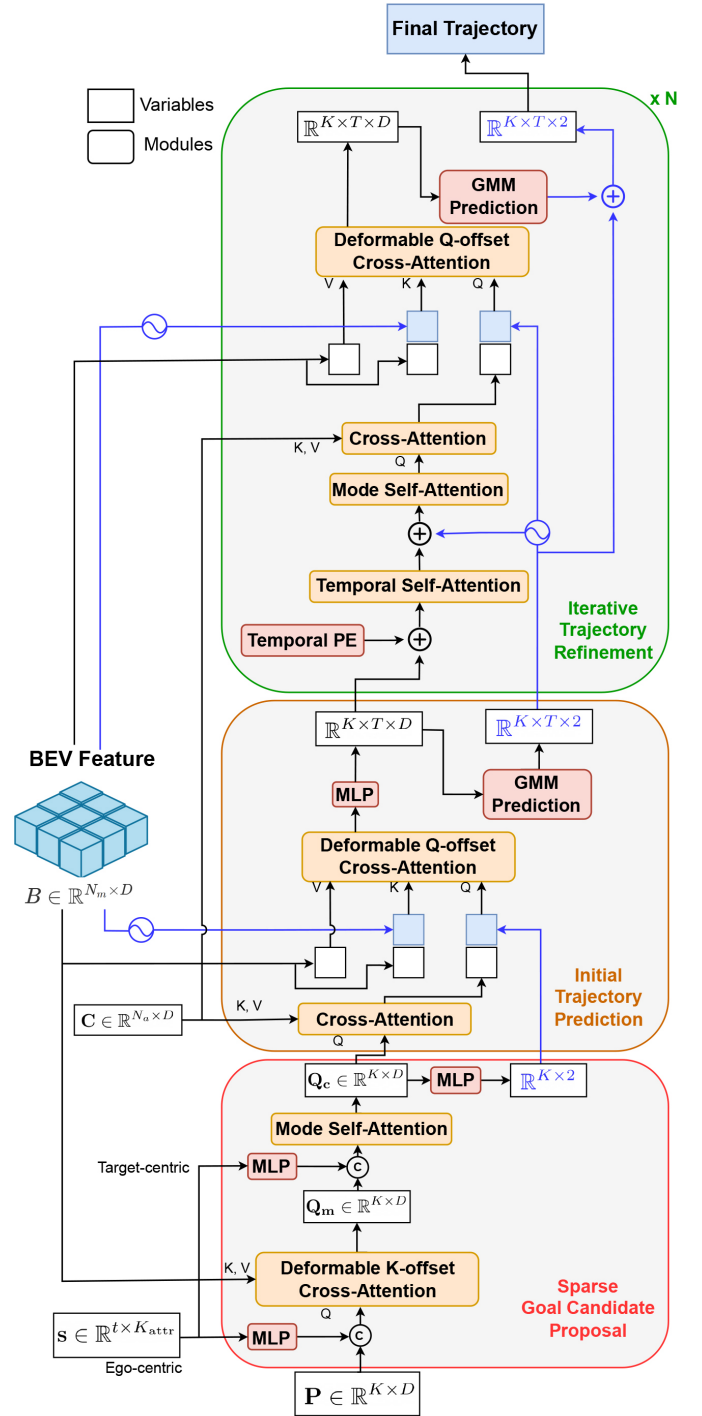


Fig. 4. Structure of the Iterative Deformable Decoder, consisting of three sub-modules for multimodal trajectory prediction: goal proposal, initial prediction, and iterative refinement. Deformable attention is used in each stage to process BEV features.

identifying navigable regions.

Another key consideration in the design of SGCP is the coordinate system in which each operation is performed. Since B is defined in the ego-centric coordinate frame, deformable cross-attention must be performed in the ego space, requiring the dynamic state s to be represented in the same coordinate frame. In contrast, goal candidates and the corresponding

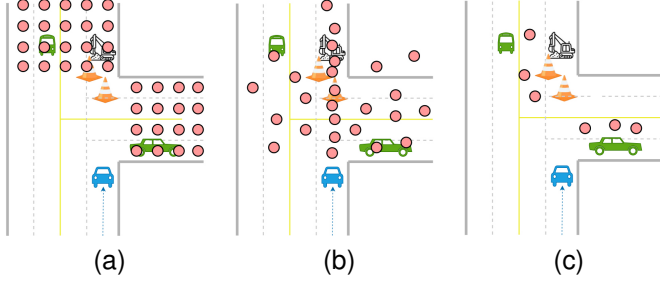


Fig. 5. Comparison of goal candidate proposal methods. (a) DenseTNT generates dense goal candidates along lanes. (b) MTR defines intention points via k-means clustering. (c) Our SGCP module predicts a sparse set of goal candidates conditioned on the agent's dynamic state and the BEV feature map.

initial trajectories of the target agent are predicted in the target-centric coordinate frame, meaning that mode self-attention must also operate in this space, with s accordingly transformed into the target agent's coordinate frame. To ensure consistency in coordinate usage throughout the decoder, we apply deformable cross-attention prior to mode self-attention. More importantly, this ordering ensures that the Q_m contains rich contextual information, which is critical both for facilitating information exchange between Q_m during mode self-attention and for assigning distinct spatial roles to each mode query.

2) *Initial Trajectory Prediction*: The *Initial Trajectory Prediction (ITP)* module is designed to generate initial trajectories from the proposed goal candidates. ITP operates as follows: First, it performs cross-attention between the content queries Q_c and the scene context feature C , incorporating interactions with surrounding agents. It then applies deformable cross-attention over the BEV feature map B , where the goal predictions from SGCP serve as reference points and offsets are computed from Q_c . By using the predicted goals as reference points, each mode can attend to road structures near its predicted destination, reducing unnecessary computation.

Following prior work [15], [21], [22], sinusoidal positional encoding is applied to the predicted goal positions, which are used as positional queries. The resulting features are passed through an MLP to expand the channel dimension to $T \times D$, and then reshaped into $\mathbb{R}^{K \times T \times D}$ introducing a temporal dimension that is maintained in subsequent modules. This temporal bottleneck strategy naturally aligns with the functional requirements of each module: the goal candidate proposal does not require temporal reasoning, whereas trajectory prediction and refinement inherently do.

Finally, the resulting embeddings are used to predict the multimodal distribution of initial trajectories via a Gaussian Mixture Model (GMM) at each time step.

3) *Iterative Trajectory Refinement*: Following the paradigm commonly adopted in detection models—where each decoder block refines the output of the previous one and uses explicit position encodings as positional queries [21], [22], [32], [33], MTR [15] extended this framework to trajectory prediction. Similarly, the *Iterative Trajectory Refinement (ITR)* module in BEVTraj adopts this paradigm to iteratively refine the initial trajectories predicted by ITP.

The ITR module operates as follows: it first applies tem-

poral self-attention and mode self-attention to the decoder embedding output from ITP, denoted as $\in \mathbb{R}^{K \times T \times D}$. It then performs cross-attention and deformable cross-attention with the scene context feature C , where offsets are derived from the query embeddings, as in ITP. Finally, refinement offsets $(\Delta x, \Delta y)$ are computed to update the trajectory predictions from the previous refinement block.

While the ITR module is structurally similar to the MTR decoder, its key distinction lies in distributing queries across future timestamps. This allows temporal self-attention to treat vectors at each time step as independent tokens, enabling better modeling of motion tendencies. Moreover, because the target agent's position at each time step is used as a reference point for deformable attention, the module can selectively retrieve time-specific contextual features from the BEV feature map B .

C. Losses

The overall training objective is defined as the sum of four loss components:

$$\mathcal{L}_{\text{total}} = \mathcal{L}_{\text{goal}} + \mathcal{L}_{\text{disp}} + \mathcal{L}_{\text{dense}} + \mathcal{L}_{\text{multi}} \quad (1)$$

Each term in Eq. (1) corresponds to a specific prediction module and is described in detail below.

1) *Goal Loss* ($\mathcal{L}_{\text{goal}}$): We generate K goal candidates $\{\hat{g}_k\}$ and supervise the one closest to the ground-truth final position g using an ℓ_2 regression loss:

$$\mathcal{L}_{\text{goal}} = \min_k \|\hat{g}_k - g\|_2^2 \quad (2)$$

2) *Displacement Loss* ($\mathcal{L}_{\text{disp}}$): Following Ye et al. [34], each goal candidate predicts its own final displacement error (FDE) as a scalar. These predictions are trained using a Smooth ℓ_1 loss:

$$\mathcal{L}_{\text{disp}} = \frac{1}{K} \sum_{k=1}^K \text{SmoothL1}(\hat{d}_k, \|\hat{g}_k - g\|_2) \quad (3)$$

3) *Dense Trajectory Loss* ($\mathcal{L}_{\text{dense}}$): To supervise dense future trajectory regression, we apply an ℓ_1 loss as proposed by Shi et al. [15]:

$$\mathcal{L}_{\text{dense}} = \|\hat{Y} - Y\|_1$$

where \hat{Y} and Y denote the predicted and ground-truth future trajectories, respectively.

4) *Multimodal Loss* ($\mathcal{L}_{\text{multi}}$): For multimodal trajectory prediction, we follow Girgis et al. [14] and adopt the combined loss $\mathcal{L}_{\text{multi}}$, which integrates four components:

$$\mathcal{L}_{\text{multi}} = \mathcal{L}_{\text{nll}} + \mathcal{L}_{\text{kl}} + \mathcal{L}_{\text{ent}} + \mathcal{L}_{\text{aux}} \quad (4)$$

These four components are computed at each decoder layer and averaged to form the final $\mathcal{L}_{\text{multi}}$. Each component is defined as follows:

- *Negative Log-Likelihood Loss* (\mathcal{L}_{nll}): Measures the likelihood of the ground-truth trajectory under the predicted mode distributions, weighted by their posterior probabilities.

- KL Divergence Loss (\mathcal{L}_{kl}): Encourages alignment between the predicted prior and posterior distributions over trajectory modes.
- Entropy Regularization (\mathcal{L}_{ent}): Promotes mode sharpness by penalizing high-entropy trajectory distributions within each mode.
- Auxiliary Displacement Loss (\mathcal{L}_{aux}): Penalizes the displacement error of the best-matching predicted mode with respect to the ground-truth.

IV. EXPERIMENTS

A. Datasets and Evaluation Metrics

1) *Datasets*: We evaluate BEVTraj on *nuScenes dataset* [35], a large-scale autonomous driving dataset collected in Boston, USA, and Singapore. It encompasses diverse driving environments, including intersections, urban streets, residential areas, and industrial zones. In this study, we focus on the trajectory prediction task, which is defined as predicting the future 6 seconds of agent motion given 2 seconds of past trajectory as input. We use the official prediction split of the dataset, consisting of approximately 32k training samples and 9k validation samples.

We also utilize the Argoverse 2 Sensor dataset [36], a large-scale autonomous driving dataset collected across six U.S. cities, including Miami, Pittsburgh, and Washington, D.C. It comprises 1,000 vehicle logs, each approximately 15 seconds long, totaling 4.2 hours of driving data. Each log contains synchronized sensor data from two 32-beam lidars and nine cameras (seven ring cameras and two stereo cameras), captured at 10 Hz and 20 Hz, respectively.

Unlike nuScenes, which provides predefined target agents, Argoverse 2 Sensor does not specify prediction targets. Therefore, we extract 28k training samples and 6k validation samples by identifying suitable target agents based on object type, motion, trajectory validity, and proximity to the ego-vehicle. Each sample consists of 2 seconds of past and 6 seconds of future trajectory, sampled at 10 Hz. This setting is aligned with the nuScenes-based setup to ensure fair comparison.

2) *Evaluation Metrics*: To assess performance, The following evaluation metrics were adopted:

- minADE (Minimum Average Displacement Error): The average Euclidean distance between the predicted trajectory and the ground-truth trajectory, computed over all future time steps. The minimum value among multiple predicted trajectories is used for evaluation, reflecting the best matching mode.
- minFDE (Minimum Final Displacement Error): The Euclidean distance between the predicted final position and the ground-truth final position. Similar to minADE, the minimum distance among all predicted trajectories is taken.
- Miss Rate: The proportion of predicted trajectories whose final displacement error exceeds a predefined threshold. Lower miss rates indicate more accurate and reliable predictions.

B. Implementation and Training

1) *Implementation Details*: For data preprocessing, agent history was normalized to the target agent's coordinate system for both datasets, following Feng et al. [37]. Additionally, for nuScenes, we interpolate the agent history from 2Hz to 10Hz to match the sampling frequency of Argoverse. To improve generalization, basic data augmentation techniques—rotation, scaling, flipping, and cropping—are applied exclusively to image inputs; no augmentation is applied to point clouds or agent trajectories. To mitigate occlusion issues, multi-sweep point clouds are aggregated and warped based on the ego vehicle's motion before being input into the model.

The overall BEVTraj architecture follows an encoder-decoder structure. Each sub-module in the Scene Context Encoder is designed as follows: the Pre-Encoder employs a temporal-social attention mechanism with two stacked layers, while the BDA module uses 256 BEV aggregate queries and applies deformable aggregation through three stacked layers. The local self-attention component consists of six layers in total.

The entire architecture uses a channel dimension of 256 for each token representation (*e.g.*, *content queries*, *positional queries*) across all attention modules.

2) *Training Details*: Prior to training for the trajectory prediction task, we pre-train the Sensor Encoder on a BEV map segmentation task to enhance its ability to capture static scene elements. The model is implemented in PyTorch and optimized using AdamW. The initial learning rate is set to 1×10^{-4} and decayed by a factor of 0.4 every 5 epochs, with a weight decay of 0.01. Dropout and layer normalization are applied to decrease overfitting. We train the model for 30 epochs with a batch size of 8 using four NVIDIA RTX 4090 GPUs. In order to jointly optimize different aspects of trajectory prediction,

our model is trained end-to-end using multiple loss functions shown in Eq.1

C. Quantitative Results

To the best of our knowledge, this study is the first to attempt trajectory prediction using only raw sensor data without relying on pre-built HD maps. In this work, we aim to compare the performance of our proposed method with approaches that utilize HD maps. Unlike pre-built HD maps, sensor-based methods are inherently limited by the range of sensor data. For example, BEVFusion [6] utilizes a coverage of up to 50m, and many BEV models adopt the same data range [29]. As illustrated in Fig.6, while pre-built HD maps can provide access to static information regardless of the vehicle's location—often using data within a ± 100 m range—real-time HD maps are constrained by sensor range and are typically generated using information within ± 50 m of the ego vehicle. Therefore, to ensure a fair comparison, we evaluate performance using HD map content limited to a ± 50 m range around the ego vehicle.

Tables I and II present a performance comparison between BEVTraj using 50m-range sensor data and prior approaches using 50 m-range of local HD maps. BEVTraj achieves strong

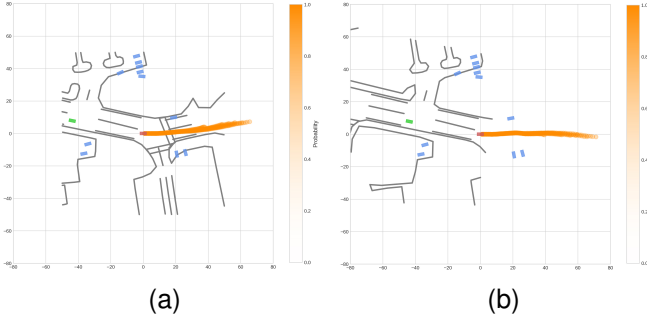


Fig. 6. Comparison of HD map ranges used in HD map-based models. Red indicates the target agent, and green indicates the ego vehicle. (a) The 50-meter map is aligned with the target agent at the center. (b) The 50-meter map is aligned with the ego vehicle at the center. In the absence of a pre-built HD map, real-time HD map construction from raw sensor data typically results in maps centered on the ego vehicle.

results in minADE₁₀, minFDE₁₀, and Miss Rate (Top-10, 2m), while delivering comparable performance across other evaluation metrics. Notably, it excels in Miss Rate, which may be attributed to the presence of multiple samples where BEVTraj generates more plausible trajectories by leveraging information available exclusively from raw sensor data.

Unlike local HD map-based methods—which require expensive and labor-intensive construction—real-time encoding from raw sensor inputs introduces inherent challenges such as calibration errors, sensor noise, and information loss due to occlusion. Moreover, raw sensor data lacks explicit semantic and topological structure, including lane connectivity and road boundaries, which are readily accessible in pre-built HD maps. Nonetheless, despite these limitations, BEVTraj proves to be a competitive alternative under realistic conditions.

TABLE I
PERFORMANCE COMPARISON OF TRAJECTORY PREDICTION ON THE VALIDATION SET OF *nuScenes* DATASET.

Method	minADE ₅ ↓	minADE ₁₀ ↓	minFDE ₁ ↓	minFDE ₁₀ ↓	Miss Rate↓
Autobot	1.9566	1.1649	8.8171	2.3294	0.3229
MTR	1.2926	1.0446	7.2689	2.2840	0.4240
Wayformer	1.4034	0.9877	7.9707	2.2483	0.3868
DeMo	1.3137	1.0424	7.1679	2.1806	0.3399
BEVTraj (Ours)	1.4556	0.9438	8.4384	2.0527	0.3082

TABLE II
PERFORMANCE COMPARISON OF TRAJECTORY PREDICTION ON THE VALIDATION SET OF *Argoverse 2 Sensor* DATASET.

Method	minADE ₅ ↓	minADE ₁₀ ↓	minFDE ₁ ↓	minFDE ₁₀ ↓	Miss Rate↓
Autobot	1.1417	0.6560	5.8954	1.3956	0.1762
MTR	0.7880	0.6799	4.6435	1.7082	0.2821
Wayformer	0.8191	0.5583	4.7608	1.3690	0.1837
DeMo	0.9000	0.6524	5.1404	1.3562	0.1776
BEVTraj (Ours)	0.9820	0.6249	5.2608	1.5832	0.1896

D. Qualitative Results

To gain deeper insights into the prediction behavior of BEVTraj beyond quantitative metrics, we perform a qualitative study across diverse driving scenarios. This analysis aims to

evaluate how effectively the model captures scene context and motion intent from raw sensor inputs.

As illustrated in Fig. 7, BEVTraj produces plausible future trajectories even under challenging conditions such as sharp curves and occluded intersections. While baseline models often generate trajectories that deviate into incorrect lanes, BEVTraj consistently preserves alignment with the correct driving lane. This suggests that raw sensor data may offer additional visual cues—such as road surface markings, physical barriers, and spatial continuity of free space—that are not explicitly represented in HD maps, which are typically constrained to predefined classes such as dividers and boundaries. We hypothesize that these fine-grained cues enable BEVTraj to more accurately infer drivable areas, thereby contributing to its superior performance in Miss Rate.

Although vectorized HD maps are compact and structurally efficient, they inherently abstract away the dense spatial details present in raw sensor data. In contrast, the BEV representation employed in BEVTraj preserves a spatial grid structure, which likely imposes stronger geometric constraints on predicted trajectories. This property appears particularly advantageous in scenarios involving sharp turns or lane merges, where precise alignment with road geometry is essential. In such cases, baseline models relying on vectorized maps often exhibit unstable lane-following behavior, whereas BEVTraj maintains more consistent and reliable performance.

This discrepancy may stem from architectural differences in the way each model encodes spatial information. For HD map-based models, the abstraction process may induce unstable activation distributions when encountering complex road geometries. In contrast, BEVTraj integrates explicit positional cues via deformable attention in a more granular and localized manner: spatial weights are not shared globally but are individually learned for each attention query.

In particular, the Iterative Deformable Decoder processes positional information independently for each predicted waypoint at every future timestamp. This design allows the model to adapt flexibly to local geometry, as each point along the predicted trajectory can selectively attend to spatial regions most relevant to its own position. Such per-timestep localization is especially advantageous in scenarios involving sharp curves or nonlinear motion, where uniform spatial treatment may degrade prediction accuracy.

Notably, BEVTraj succeeds in generating trajectories that align with implicit lane geometry and obstacle boundaries, even in the absence of explicit HD map information. These findings underscore the advantage of directly modeling dense features from raw sensor data, particularly in spatially complex environments where vectorized map representations may fall short.

E. Ablation Study

We conducted an ablation study to evaluate the contribution of each module within BEVTraj to trajectory prediction performance. All experimental conditions follow the setup described in Section IV-A, except for the inclusion or removal of the target module.

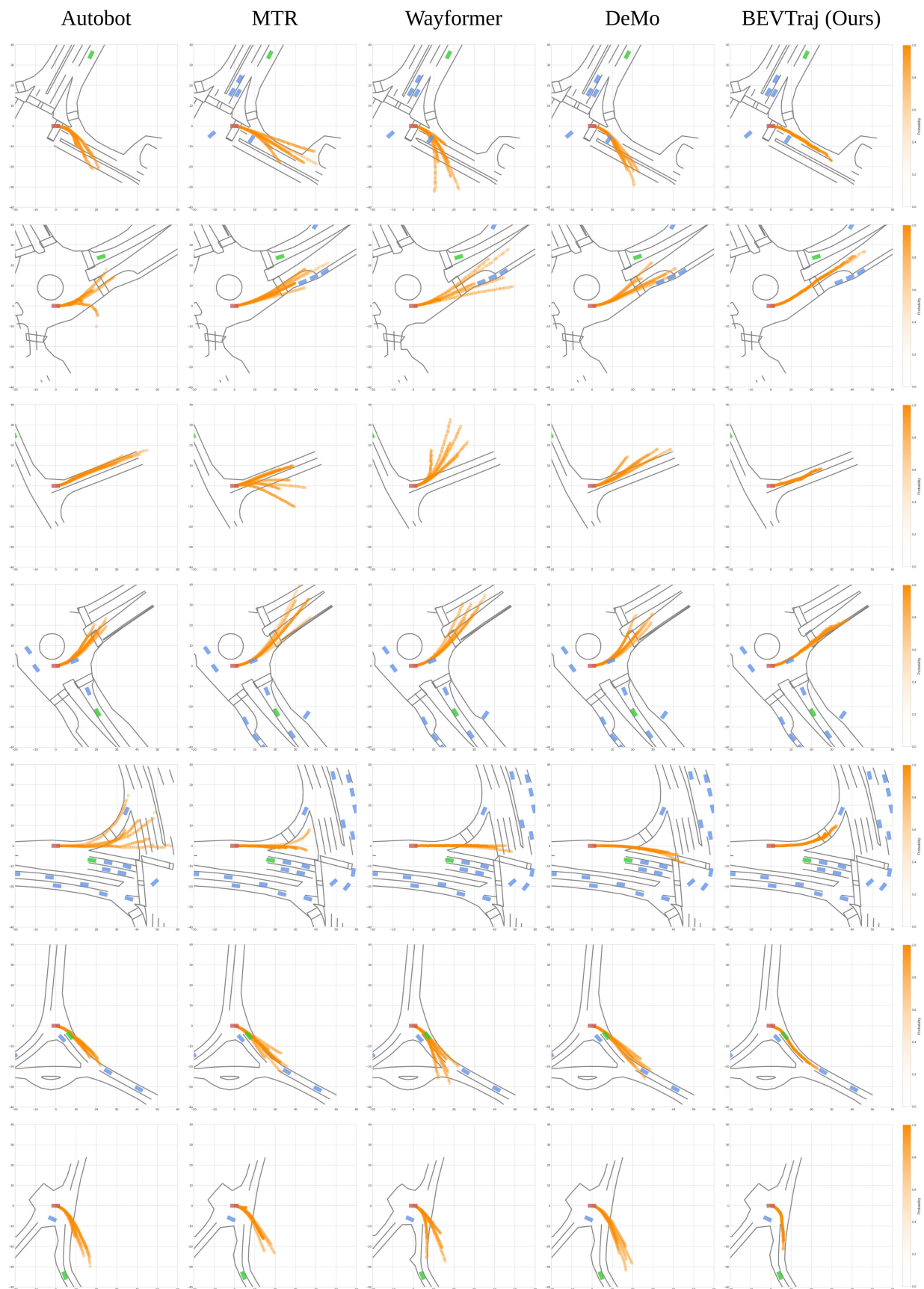


Fig. 7. Qualitative comparison in diverse driving scenarios. BEVTraj shows consistently accurate, lane-aligned predictions under complex conditions such as sharp turns and occlusions.

1) *Pre-Encoder*: We assessed the impact of the Pre-Encoder by comparing models with and without this component. As discussed in Section III-B, our model adopts a temporal bottleneck strategy, in which the temporal dimension is first compressed and later reintroduced during trajectory decoding. This design enables the model to reduce computational complexity during scene encoding while preserving essential temporal information for downstream prediction. Since both BEVTraj and MTR adopt temporal compression in their architectures (e.g., *max pooling* in MTR), they provide a meaningful basis for assessing the effectiveness of early temporal modeling prior to compression.

As shown in Table III, incorporating the Pre-Encoder improves all evaluation metrics except Miss Rate, with the most significant gain observed in **minFDE**. These findings indicate that applying temporal and social attention prior to temporal compression is effective in enhancing trajectory prediction performance. Specifically, temporal self-attention captures motion trends over time, while social attention models inter-agent interactions occurring within the same timestamp. The latter is particularly important, as it enables the model to capture fine-grained relational dependencies before temporal resolution is reduced.

This approach contrasts with modeling such interactions after temporal compression, where important short-term relational cues may have already been lost. By incorporating the Pre-Encoder, BEVTraj achieves a favorable balance between prediction accuracy and parameter efficiency, offering a design paradigm that may generalize to other models employing temporal bottleneck structures (e.g., MTR).

2) *Sparse Goal Candidate Proposal*: The SGCP module generates goal candidates that serve as initial endpoints for trajectory prediction and are iteratively refined through subsequent decoder layers. To assess its impact, we replaced SGCP with a variant that employs learnable queries without explicit conditioning on the target agent’s state or spatial context. As shown in Table III, incorporating SGCP consistently outperforms the baseline across all metrics, with the most significant improvement observed in **minFDE**, indicating enhanced accuracy in endpoint prediction within each mode.

This performance gain can be attributed to the SGCP’s architecture, which generates goal candidates based solely on the dynamic state of the target agent and static scene elements such as road topology—without leveraging inter-agent interactions or the scene context feature **C**. Compared to full trajectory prediction, which requires reasoning over multi-agent dynamics and long temporal horizons, goal prediction is a simpler sub-task. Solving this sub-task early enables the model to encode the target agent’s intention into the content query \mathbf{Q}_e as prior knowledge. Furthermore, the predicted goal candidates provide spatial anchors for the Initial Trajectory Prediction (ITP) module, helping downstream components align their predictions with more semantically plausible destinations.

F. Discussion

1) *Effect of Map Range on Prediction Performance*: As discussed in Section IV-C, in the absence of pre-built HD maps,

real-time HD map construction is inherently constrained by the sensor’s perceptual range. To examine the implications of this limitation, we analyze how the performance of HD map-based models varies with respect to map range, as illustrated in Figs. 8 and 9 and Tables IV and V. Here, the map range is defined relative to the ego vehicle’s position at the current timestamp. As the spatial range of the map increases, performance generally improves across most metrics for the majority of models, indicating that access to a wider spatial context enhances predictive capability.

To better assess the models’ ability to handle challenging prediction scenarios under different map ranges, we slightly modified the target agent selection criteria for the Argoverse 2 Sensor experiments. In particular, we excluded agents that are nearly stationary or moving in a straight line, as trajectory prediction becomes more difficult when agents move at higher speeds or make sharp turns. This adjustment reduces the number of easy cases in the evaluation set, resulting in overall higher error values in Table II compared to those reported in Table II, regardless of model type.

Although this trend generally holds, there are notable deviations, where a smaller map range yields better results or an extended range leads to degraded performance. These exceptions suggest that the optimal spatial extent of static map information may be influenced by model architecture or its capacity to encode contextual cues. Moreover, although this study employs ground-truth HD maps to isolate the effects of map range, real-world deployments must also account for the variability in the accuracy of real-time HD map construction, which may deteriorate as spatial coverage increases. These observations underscore the need for future work to jointly consider model-specific context integration capabilities and the reliability of map construction across varying spatial ranges.

The spatial constraints imposed by the sensor’s perceptual field apply not only to real-time HD map construction but also to BEVTraj. These findings indicate that BEVTraj performance may further improve with extended sensor range, as its deformable attention mechanism allows the model to selectively focus on informative regions within the BEV feature space. Future advancements in sensing technology or cooperative infrastructure—such as V2X communication—could expand the observable environment, thereby enhancing both perception and prediction capabilities.

2) *Ego-Vehicle Trajectory Prediction*: In addition to forecasting the trajectories of surrounding agents, we also evaluated our model’s performance in predicting the ego vehicle’s future motion. Unlike conventional baseline models that rely solely on HD maps and historical trajectories, our approach leverages raw sensor inputs—such as LiDAR and camera data—to construct a richer and more adaptive representation of the scene.

As shown in Table VI, our model achieves comparable or slightly improved performance in ego trajectory prediction relative to baseline methods. This performance gain can be attributed to the model’s capacity to incorporate dynamic environmental cues and agent interactions, which are often underrepresented in HD map-based frameworks. Sensor-derived BEV representations offer real-time insights into nuanced

TABLE III
ABLATION STUDY ON THE IMPACT OF DIFFERENT COMPONENTS.

Method	Pre-Encoder	SGCP	minADE ₅ ↓	minADE ₁₀ ↓	minFDE ₁ ↓	minFDE ₁₀ ↓	Miss Rate ↓
MTR	X	-	1.4204	1.1222	8.1122	2.4326	0.4443
	O	-	1.3718	1.1146	7.5796	2.3875	0.4156
BEVTraj	X	O	1.6501	1.0356	8.7623	2.3186	0.2852
	O	X	1.7060	1.0790	9.4390	2.4280	0.3603
	O	O	1.4556	0.9438	8.4384	2.0527	0.3082

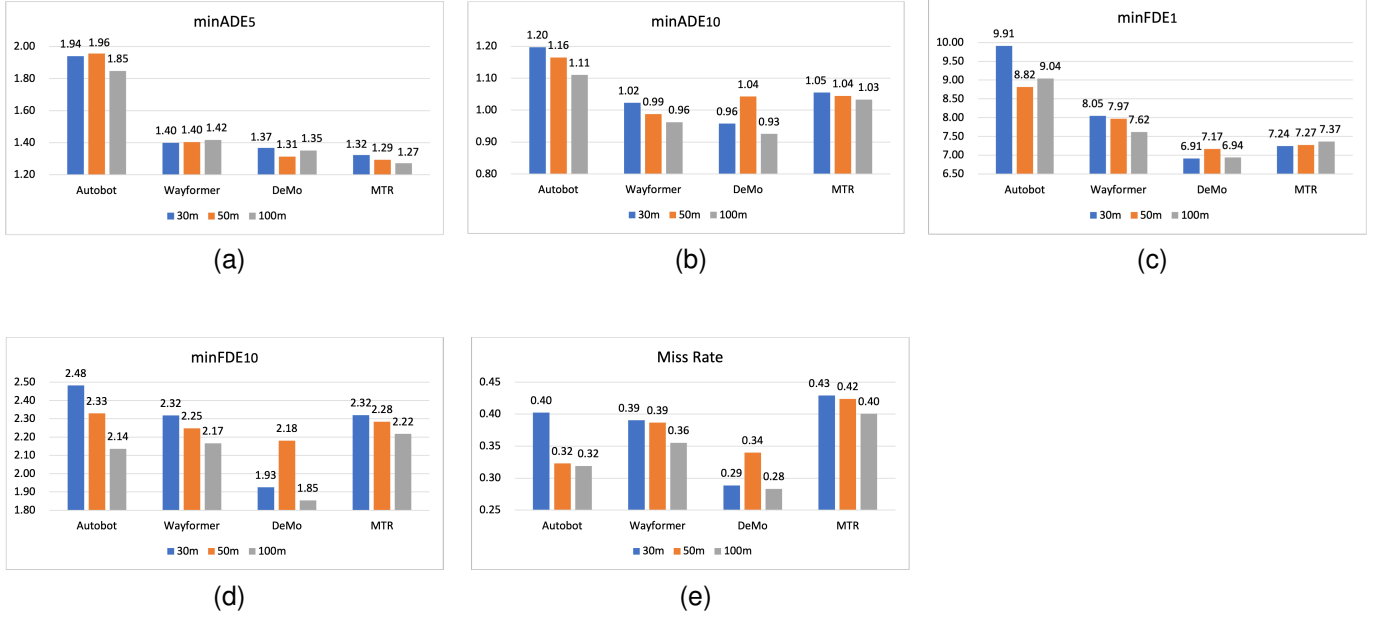


Fig. 8. Performance comparison of HD map-based models on the validation set of the *nuScenes* dataset. (a) minADE₅. (b) minADE₁₀. (c) minFDE₁. (d) minFDE₁₀. (e) Miss rate.

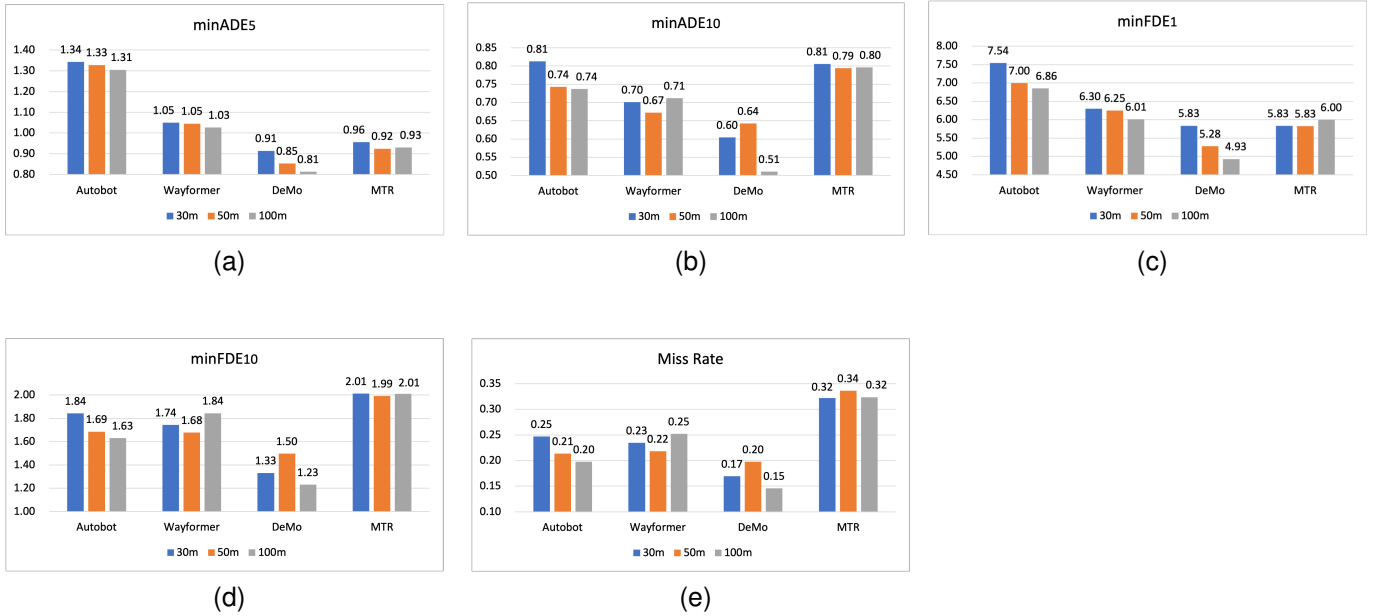


Fig. 9. Performance comparison of HD map-based models on the validation set of the *Argoverse 2 Sensor* dataset. (a) minADE₅. (b) minADE₁₀. (c) minFDE₁. (d) minFDE₁₀. (e) Miss rate.

scene dynamics and unexpected events within the ego vehicle's perceptual field, thereby enhancing the model's understanding

of driving intent and scene context. This results in more accurate and responsive ego trajectory prediction.

TABLE IV

PERFORMANCE COMPARISON OF HD MAP-BASED MODELS ON THE *nuScenes* VALIDATION SET. THE NUMBER IN PARENTHESES INDICATES THE SPATIAL RANGE (IN METERS) OF THE INPUT HD MAP (*i.e.*, 30M, 50M, 100M).

Method	minADE ₅ ↓	minADE ₁₀ ↓	minFDE ₁ ↓	minFDE ₁₀ ↓	Miss Rate↓
Autobot (30)	1.9407	1.1969	9.9123	2.4823	0.4023
Autobot (50)	1.9566	1.1649	8.8171	2.3294	0.3229
Autobot (100)	1.8475	1.1100	9.0446	2.1356	0.3190
MTR (30)	1.3228	1.0547	7.2409	2.3198	0.4291
MTR (50)	1.2926	1.0446	7.2689	2.2840	0.4240
MTR (100)	1.2722	1.0332	7.3652	2.2170	0.4007
Wayformer (30)	1.3983	1.0226	8.0459	2.3181	0.3903
Wayformer (50)	1.4034	0.9877	7.9707	2.2483	0.3868
Wayformer (100)	1.4166	0.9620	7.6164	2.1658	0.3552
DeMo (30)	1.3669	0.9575	6.9147	1.9255	0.2886
DeMo (50)	1.3137	1.0424	7.1679	2.1806	0.3399
DeMo (100)	1.3518	0.9254	6.9370	1.8536	0.2833

TABLE V

PERFORMANCE COMPARISON OF HD MAP-BASED MODELS ON THE *Argoverse 2 Sensor* VALIDATION SET. THE NUMBER IN PARENTHESES INDICATES THE SPATIAL RANGE (IN METERS) OF THE INPUT HD MAP (*i.e.*, 30M, 50M, 100M).

Method	minADE ₅ ↓	minADE ₁₀ ↓	minFDE ₁ ↓	minFDE ₁₀ ↓	Miss Rate↓
Autobot (30)	1.3426	0.8128	7.5449	1.8431	0.2470
Autobot (50)	1.3284	0.7430	6.9975	1.6861	0.2136
Autobot (100)	1.3052	0.7370	6.8554	1.6304	0.1977
MTR (30)	0.9558	0.8055	5.8315	2.0128	0.3221
MTR (50)	0.9243	0.7944	5.8264	1.9926	0.3361
MTR (100)	0.9299	0.7961	5.9988	2.0115	0.3237
Wayformer (30)	1.0499	0.7009	6.2962	1.7431	0.2344
Wayformer (50)	1.0454	0.6721	6.2511	1.6775	0.2181
Wayformer (100)	1.0268	0.7122	6.0104	1.8444	0.2521
DeMo (30)	0.9142	0.6046	5.8348	1.3308	0.1692
DeMo (50)	0.8528	0.6426	5.2801	1.4964	0.1976
DeMo (100)	0.8133	0.5107	4.9291	1.2306	0.1455

Furthermore, the proposed model architecture is inherently extensible beyond trajectory prediction, offering a natural pathway toward motion planning applications. By leveraging real-time perception to infer feasible and context-aware future trajectories, the framework can be seamlessly integrated into downstream decision-making and path planning modules, underscoring its potential as a unified solution that bridges the gap between perception and planning in autonomous driving systems.

TABLE VI

EGO-VEHICLE TRAJECTORY FORECASTING RESULTS ON THE VALIDATION SET OF THE *nuScenes Dataset*. BEVTRAJ ACHIEVES COMPARABLE PERFORMANCE TO HD MAP-BASED BASELINES UNDER THE SAME SPATIAL COVERAGE CONSTRAINT.

Method	minADE ₅ ↓	minADE ₁₀ ↓	minFDE ₁ ↓	minFDE ₁₀ ↓	Miss Rate↓
Autobot	1.1059	0.9432	6.9950	2.1440	0.3313
MTR	0.9528	0.8958	6.0512	2.0596	0.3649
Wayformer	1.0501	0.6827	6.5616	1.4936	0.2131
DeMo	1.0720	0.7986	5.6852	1.8206	0.2490
BEVTraj (Ours)	1.1694	0.6751	6.3221	1.3170	0.1374

V. CONCLUSION

In this paper, we introduced Bird’s-Eye View Trajectory Prediction (BEVTraj), a novel end-to-end framework that eliminates dependence on pre-built HD maps by directly leveraging

real-time sensor data. BEVTraj effectively captures dynamic environmental changes while maintaining high prediction accuracy. It utilizes a BEV-based representation to encode spatial and contextual information, and employs deformable attention to selectively extract salient features from dense BEV inputs, enabling accurate and consistent trajectory prediction.

Moreover, the proposed Sparse Goal Candidate Proposal (SGCP) module improves efficiency by removing the need for post-processing operations. Extensive experiments demonstrate that BEVTraj achieves performance competitive with HD map-based methods, while offering enhanced adaptability across diverse driving scenarios. These findings validate the feasibility of map-free trajectory prediction and highlight BEVTraj’s potential as a scalable and flexible solution for autonomous driving.

For future work, we aim to extend the framework by incorporating BEV feature-based object detection and tracking modules, enabling the joint processing of static and dynamic scene information within a unified representation space. Additionally, enhancing the temporal modeling capacity of BEV features through recurrent architectures or cross-sweep fusion techniques may further improve the model’s ability to capture long-term motion patterns. Investigating adaptive BEV grid structures could also help mitigate spatial limitations, allowing for more flexible and fine-grained trajectory prediction. We anticipate that these improvements will contribute to a more comprehensive and robust trajectory prediction system.

Furthermore, the techniques developed in this work are not limited to autonomous driving but can also be applied to broader domains, such as surveillance systems—where monitoring vehicle and human activities is critical for safety [38]–[42],—and robotics, where accurate trajectory prediction is essential for tasks such as human–robot interaction and navigation in dynamic environments [43].

ACKNOWLEDGMENTS

This work was supported by Artificial intelligence industrial convergence cluster development project funded by the Ministry of Science and ICT(MSIT, Korea) & Gwangju Metropolitan City and the National Research Foundation of Korea (NRF) grant funded by the Korea government (MSIT). (No. 2020R1A2C1102767)

REFERENCES

- [1] Q. Li, Y. Wang, Y. Wang, and H. Zhao, “Hdmapnet: An online hd map construction and evaluation framework,” in *2022 International Conference on Robotics and Automation (ICRA)*. IEEE, 2022, pp. 4628–4634.
- [2] B. Liao, S. Chen, X. Wang, T. Cheng, Q. Zhang, W. Liu, and C. Huang, “Maptr: Structured modeling and learning for online vectorized hd map construction,” *arXiv preprint arXiv:2208.14437*, 2022.
- [3] S. Choi, J. Kim, H. Shin, and J. W. Choi, “Mask2map: Vectorized hd map construction using bird’s eye view segmentation masks,” in *European Conference on Computer Vision*. Springer, 2024, pp. 19–36.
- [4] J. Philion and S. Fidler, “Lift, splat, shoot: Encoding images from arbitrary camera rigs by implicitly unprojecting to 3d,” in *Computer Vision—ECCV 2020: 16th European Conference, Glasgow, UK, August 23–28, 2020, Proceedings, Part XIV 16*. Springer, 2020, pp. 194–210.

- [5] Z. Li, W. Wang, H. Li, E. Xie, C. Sima, T. Lu, Q. Yu, and J. Dai, "Bevformer: Learning bird's-eye-view representation from lidar-camera via spatiotemporal transformers," *IEEE Transactions on Pattern Analysis and Machine Intelligence*, 2024.
- [6] Z. Liu, H. Tang, A. Amini, X. Yang, H. Mao, D. L. Rus, and S. Han, "Bevfusion: Multi-task multi-sensor fusion with unified bird's-eye view representation," in *2023 IEEE international conference on robotics and automation (ICRA)*. IEEE, 2023, pp. 2774–2781.
- [7] T. Phan-Minh, E. C. Grigore, F. A. Boulton, O. Beijbom, and E. M. Wolff, "Covernet: Multimodal behavior prediction using trajectory sets," in *Proceedings of the IEEE/CVF conference on computer vision and pattern recognition*, 2020, pp. 14 074–14 083.
- [8] Y. Chai, B. Sapp, M. Bansal, and D. Anguelov, "Multipath: Multiple probabilistic anchor trajectory hypotheses for behavior prediction," *arXiv preprint arXiv:1910.05449*, 2019.
- [9] H. Cui, V. Radosavljevic, F.-C. Chou, T.-H. Lin, T. Nguyen, T.-K. Huang, J. Schneider, and N. Djuric, "Multimodal trajectory predictions for autonomous driving using deep convolutional networks," in *2019 international conference on robotics and automation (icra)*. IEEE, 2019, pp. 2090–2096.
- [10] M. Liang, B. Yang, R. Hu, Y. Chen, R. Liao, S. Feng, and R. Urtasun, "Learning lane graph representations for motion forecasting," in *Computer Vision—ECCV 2020: 16th European Conference, Glasgow, UK, August 23–28, 2020, Proceedings, Part II 16*. Springer, 2020, pp. 541–556.
- [11] S. Afshar, N. Deo, A. Bhagat, T. Chakraborty, Y. Shao, B. R. Budharaju, A. Deshpande, and H. C. Motional, "Pbp: Path-based trajectory prediction for autonomous driving," in *2024 IEEE International Conference on Robotics and Automation (ICRA)*. IEEE, 2024, pp. 12 927–12 934.
- [12] J. Gao, C. Sun, H. Zhao, Y. Shen, D. Anguelov, C. Li, and C. Schmid, "Vectornet: Encoding hd maps and agent dynamics from vectorized representation," in *Proceedings of the IEEE/CVF conference on computer vision and pattern recognition*, 2020, pp. 11 525–11 533.
- [13] A. Vaswani, "Attention is all you need," *Advances in Neural Information Processing Systems*, 2017.
- [14] R. Girgis, F. Golemo, F. Codevilla, M. Weiss, J. A. D'Souza, S. E. Kahou, F. Heide, and C. Pal, "Latent variable sequential set transformers for joint multi-agent motion prediction," *arXiv preprint arXiv:2104.00563*, 2021.
- [15] S. Shi, L. Jiang, D. Dai, and B. Schiele, "Motion transformer with global intention localization and local movement refinement," *Advances in Neural Information Processing Systems*, vol. 35, pp. 6531–6543, 2022.
- [16] N. Nayakanti, R. Al-Rfou, A. Zhou, K. Goel, K. S. Refaat, and B. Sapp, "Wayformer: Motion forecasting via simple & efficient attention networks," in *2023 IEEE International Conference on Robotics and Automation (ICRA)*. IEEE, 2023, pp. 2980–2987.
- [17] C. Feng, H. Zhou, H. Lin, Z. Zhang, Z. Xu, C. Zhang, B. Zhou, and S. Shen, "Macformer: Map-agent coupled transformer for real-time and robust trajectory prediction," *IEEE Robotics and Automation Letters*, 2023.
- [18] Z. Zhou, L. Ye, J. Wang, K. Wu, and K. Lu, "Hivt: Hierarchical vector transformer for multi-agent motion prediction," in *Proceedings of the IEEE/CVF Conference on Computer Vision and Pattern Recognition*, 2022, pp. 8823–8833.
- [19] Z. Zhou, J. Wang, Y.-H. Li, and Y.-K. Huang, "Query-centric trajectory prediction," in *Proceedings of the IEEE/CVF Conference on Computer Vision and Pattern Recognition*, 2023, pp. 17 863–17 873.
- [20] J. Gu, C. Sun, and H. Zhao, "Densetnt: End-to-end trajectory prediction from dense goal sets," in *Proceedings of the IEEE/CVF International Conference on Computer Vision*, 2021, pp. 15 303–15 312.
- [21] D. Meng, X. Chen, Z. Fan, G. Zeng, H. Li, Y. Yuan, L. Sun, and J. Wang, "Conditional detr for fast training convergence," in *Proceedings of the IEEE/CVF international conference on computer vision*, 2021, pp. 3651–3660.
- [22] S. Liu, F. Li, H. Zhang, X. Yang, X. Qi, H. Su, J. Zhu, and L. Zhang, "Dab-detr: Dynamic anchor boxes are better queries for detr," *arXiv preprint arXiv:2201.12329*, 2022.
- [23] S. Choi, J. Kim, J. Yun, and J. W. Choi, "R-pred: Two-stage motion prediction via tube-query attention-based trajectory refinement," in *Proceedings of the IEEE/CVF International Conference on Computer Vision*, 2023, pp. 8525–8535.
- [24] Y. Hu, J. Yang, L. Chen, K. Li, C. Sima, X. Zhu, S. Chai, S. Du, T. Lin, W. Wang *et al.*, "Planning-oriented autonomous driving," in *Proceedings of the IEEE/CVF Conference on Computer Vision and Pattern Recognition*, 2023, pp. 17 853–17 862.
- [25] S. Chen, B. Jiang, H. Gao, B. Liao, Q. Xu, Q. Zhang, C. Huang, W. Liu, and X. Wang, "Vadv2: End-to-end vectorized autonomous driving via probabilistic planning," *arXiv preprint arXiv:2402.13243*, 2024.
- [26] Z. Chen, M. Ye, S. Xu, T. Cao, and Q. Chen, "Ppad: Iterative interactions of prediction and planning for end-to-end autonomous driving," in *European Conference on Computer Vision*. Springer, 2024, pp. 239–256.
- [27] W. Zheng, R. Song, X. Guo, C. Zhang, and L. Chen, "Genad: Generative end-to-end autonomous driving," in *European Conference on Computer Vision*. Springer, 2024, pp. 87–104.
- [28] A. Hu, Z. Murez, N. Mohan, S. Dudas, J. Hawke, V. Badrinarayanan, R. Cipolla, and A. Kendall, "Fiery: Future instance prediction in bird's-eye view from surround monocular cameras," in *Proceedings of the IEEE/CVF International Conference on Computer Vision*, 2021, pp. 15 273–15 282.
- [29] Y. Zhang, Z. Zhu, W. Zheng, J. Huang, G. Huang, J. Zhou, and J. Lu, "Beverse: Unified perception and prediction in birds-eye-view for vision-centric autonomous driving," *arXiv preprint arXiv:2205.09743*, 2022.
- [30] S. Fang, Z. Wang, Y. Zhong, J. Ge, and S. Chen, "Tbp-former: Learning temporal bird's-eye-view pyramid for joint perception and prediction in vision-centric autonomous driving," in *Proceedings of the IEEE/CVF Conference on Computer Vision and Pattern Recognition*, 2023, pp. 1368–1378.
- [31] C. R. Qi, H. Su, K. Mo, and L. J. Guibas, "Pointnet: Deep learning on point sets for 3d classification and segmentation," in *Proceedings of the IEEE conference on computer vision and pattern recognition*, 2017, pp. 652–660.
- [32] X. Zhu, W. Su, L. Lu, B. Li, X. Wang, and J. Dai, "Deformable detr: Deformable transformers for end-to-end object detection," *arXiv preprint arXiv:2010.04159*, 2020.
- [33] H. Zhang, F. Li, S. Liu, L. Zhang, H. Su, J. Zhu, L. M. Ni, and H.-Y. Shum, "Dino: Detr with improved denoising anchor boxes for end-to-end object detection," *arXiv preprint arXiv:2203.03605*, 2022.
- [34] M. Ye, T. Cao, and Q. Chen, "Tpcn: Temporal point cloud networks for motion forecasting," in *Proceedings of the IEEE/CVF Conference on Computer Vision and Pattern Recognition*, 2021, pp. 11 318–11 327.
- [35] H. Caesar, V. Bankiti, A. H. Lang, S. Vora, V. E. Liong, Q. Xu, A. Krishnan, Y. Pan, G. Baldan, and O. Beijbom, "nusenes: A multimodal dataset for autonomous driving," in *Proceedings of the IEEE/CVF conference on computer vision and pattern recognition*, 2020, pp. 11 621–11 631.
- [36] B. Wilson, W. Qi, T. Agarwal, J. Lambert, J. Singh, S. Khandelwal, B. Pan, R. Kumar, A. Hartnett, J. K. Pontes *et al.*, "Argoverse 2: Next generation datasets for self-driving perception and forecasting," *arXiv preprint arXiv:2301.00493*, 2023.
- [37] L. Feng, M. Bahari, K. M. B. Amor, É. Zablocki, M. Cord, and A. Alahi, "Unitraj: A unified framework for scalable vehicle trajectory prediction," in *European Conference on Computer Vision*. Springer, 2024, pp. 106–123.
- [38] S. Lee, T. Woo, and S. H. Lee, "Multi-attention-based soft partition network for vehicle re-identification," *Journal of Computational Design and Engineering*, vol. 10, no. 2, pp. 488–502, 02 2023. [Online]. Available: <https://doi.org/10.1093/jcde/qwad014>
- [39] S. Lee, E. Park, H. Yi, and S. H. Lee, "StRDAN: Synthetic-to-real domain adaptation network for vehicle re-identification," in *Proceedings of the IEEE/CVF Conference on Computer Vision and Pattern Recognition (CVPR)*, 2020, pp. 608–609.
- [40] S. Lee, T. Woo, and S. H. Lee, "SBNNet: Segmentation-based network for natural language-based vehicle search," in *Proceedings of the IEEE/CVF Conference on Computer Vision and Pattern Recognition (CVPR)*, 2021, pp. 4054–4060.
- [41] H. Eom and S. H. Lee, "Mode confusion of human-machine interfaces for automated vehicles," *Journal of Computational Design and Engineering*, vol. 9, no. 5, pp. 1995–2009, 2022.
- [42] R. Huang, H. Xue, M. Pagnucco, F. D. Salim, and Y. Song, "Vision-based multi-future trajectory prediction: A survey," *IEEE Transactions on Neural Networks and Learning Systems*, pp. 1–18, 2025.
- [43] A. Rudenko, L. Palmieri, M. Herman, K. M. Kitani, D. M. Gavrila, and K. O. Arras, "Human motion trajectory prediction: A survey," *The International Journal of Robotics Research*, vol. 39, no. 8, pp. 895–935, 2020.



in research projects on self-driving perception and prediction models. He has also contributed to the academic community through competitions and workshops.

Minsang Kong is with the Department of Automobile and IT Convergence, Kookmin University, Seoul, South Korea. His research interests include autonomous driving technology, deep learning-based perception, trajectory prediction, and multi-agent behavior modeling. He is particularly interested in sensor fusion, object detection, and the application of artificial intelligence in real-world autonomous systems. He has received multiple awards for his research contributions and has actively participated



models. He has also contributed to the academic community through competitions and workshops.

Myeongjun Kim is with the Department of Automobile and IT Convergence, Kookmin University, Seoul, South Korea. His research interests include autonomous driving technology, deep learning-based perception, and multimodal trajectory prediction. He is particularly interested in sensor fusion, object detection, and end-to-end autonomous driving. He has received multiple awards for his research contributions and has actively participated in research projects on self-driving perception and prediction



Sanggu Kang is with the Department of Automotive Engineering, Kookmin University, Seoul, South Korea. His research interests include artificial intelligence, autonomous driving, and deep learning-based computer vision, with a focus on object detection, V2X datasets, and trajectory prediction. He has contributed to sensor fusion and object detection for autonomous driving systems and participated in the DriveX Challenge at CVPR, where he received a third-place award.



Sang Hun Lee received the B.S., M.S., and Ph.D. degrees in Mechanical Design and Production Engineering from Seoul National University, Seoul, South Korea, in 1986, 1988, and 1993, respectively. From 1993 to 1995, he was a Senior Researcher with the Research Center of Sindo Ricoh Co. Since 1996, he has been a Professor with both the Department of Automotive Engineering and the Graduate School of Automobile and Mobility, Kookmin University, Seoul, South Korea.

Dr. Lee has authored more than 70 papers in international journals and conference proceedings. He currently serves as a Co-Editor-in-Chief of the Journal of Computational Design and Engineering. His research interests include intelligent vehicles, human-centered autonomous systems, human-machine interaction, computer-aided design, and the application of artificial intelligence in industry.